

Tunneling of localized excitations: giant enhancement due to fluctuations

S. Flach¹, V. Fleurov² and A. A. Ovchinnikov¹
¹ *MPIPKS, Nöthnitzer Str. 38, 01187 Dresden, Germany*
² *Beverly and Raymond Sackler Faculty of Exact Sciences
School of Physics and Astronomy, Tel Aviv University
Tel Aviv 69978, Israel*
(November 21, 2018)

We consider the tunneling of localized excitations (many boson bound states) in the presence of a bosonic bath. We show both analytically and numerically that the bath influence results in a dramatical enhancement of the amplitude of the excitation tunneling. The order of the bosonic flow in the course of the tunneling process is obtained. On the background of the giant tunneling enhancement we observe and describe additional resonant enhancement and *suppression* of tunneling due to avoided level crossings.

I. INTRODUCTION

Tunneling properties of, e.g., local bond excitations in molecules, of bound states in quantum lattices or of large spins in the presence of anisotropy fields share a lot of similarities of corresponding model approaches and technical treatments. Despite the amount of published work this field lacks complete understanding. Especially intriguing are the relation to so-called dynamical tunneling in phase space [1], the influence of heat bath coupling [2,3], the exact computation of tunneling probabilities [4,5], to name a few.

To study different aspects of the problem it is helpful to formulate a model which shares most of the needed properties, and is numerically solvable (because it is typically hard to obtain exact analytical results).

In the present paper we will study the tunneling of multi boson bound states in a model which we believe possesses all necessary qualitative ingredients needed for the understanding of a more general case.

The Hamiltonian of the model is given by

$$H = \frac{1}{2} \left[(a_1^\dagger a_1)^2 + (a_2^\dagger a_2)^2 \right] + C (a_1^\dagger a_2 + a_1 a_2^\dagger) + \delta (a_1^\dagger a_3 + a_1 a_3^\dagger + a_2^\dagger a_3 + a_2 a_3^\dagger) \quad (1.1)$$

Here the operators a_l, a_l^\dagger ($l = 1, 2, 3$) are bosonic annihilation and creation operators with standard commutation relations $[a_l, a_m^\dagger] = \delta_{lm}$. Note that (1.1) is invariant under permutation of site 1 with site 2.

Equation (1.1) describes, e.g., a three site (or bond) molecule, i.e. a trimer [7]. It could also serve as a model for tunneling in a dimer [8] (just sites 1 and 2) under the simultaneous influence of a heat (or energy) bath on site 3, coupled to the symmetric modes of the dimer. It may be used for a study of excitations in H_2O molecules, where the two $O-H$ stretching modes (dimer) are additionally coupled to the relative angle between the two bonds (third site) [6].

Finally (1.1) may be transformed into a model of a spin with local anisotropy and external field (site 3) coupled to a bosonic field (using Schwinger bosons for sites 1 and 2). The coupling is such that the total spin length will not be conserved, but may fluctuate. The dimer limit $\delta = 0$ may be represented as a spin length conserving model with the Hamiltonian $H_s = S_z^2 + 2CS_x$ [9,10].

Model (1.1) conserves in addition to the energy also the total particle number b which is an eigenvalue of the total number operator B

$$B = n_1 + n_2 + n_3 \quad , \quad n_l = a_l^\dagger a_l \quad . \quad (1.2)$$

Note that due to this conservation the infinite dimensional Hilbert space decomposes into an infinite set of finite dimensional orthogonal subspaces, each with a given total particle number. Consequently numerical evaluations will always translate into diagonalizations of finite matrices, without worrying about truncation errors. The classical limit is obtained by replacing the operators a_l with complex scalars Ψ_l (Hermitian conjugation is replaced by complex conjugation).

Besides the above mentioned general interest in such kinds of model we want to give some additional reasons for studying of (1.1). During the past decade we witnessed an explosion of interest to a new class of excitations in lattice models. These models are typically described by Hamiltonian equations of motion of degrees of freedom associated with lattice points of spatial periodic lattices. In the presence of interaction between these degrees of freedom, when considering linear equations of motion, the translational symmetry of the underlying lattice allows one to obtain delocalized plane wave solutions (phonons, magnons and other *whateverons*. The spectra of these excitations have finite upper bounds due to the discreteness of the system. If instead considering rather arbitrary additional nonlinearities in the equations of motion, a new generic type of solutions appears: **discrete breathers** [11]. These discrete breather solutions are time-periodic spatially localized excitations and appear in one-parameter families. The discrete breather concept can be easily extended to dissipative systems [12].

Much more complicated is the quantization of these excitations. The question arises which eigenstates of the quantum Hamiltonian operator correspond to classical discrete breathers. Intuition leads to the conclusion that one should search for multi *whateveron* bound states [13]. One signature should be the appearance of extremely narrow quasiparticle bands in the high energy sector. 'Quasiparticle' stands for the need of just one wave vector which labels the states of the quantum breather band (as opposed to many wave vectors which label many *whateveron* continua) [14,15]. This view is supported by the consideration of a (semiclassical) tunneling process of a discrete breather, which implicitly assumes that the quantum system may support coherent tunneling of localized excitations similar to a (quasi)particle [16]. 'Extremely narrow' could have different meanings. In the best case these bands should be much narrower than the mean level spacing in the given energy sector. This seems to be not so simple owing to the increase of the density of states when going up in energy. Another aspect of 'narrow' means weak interaction with nearby lying states.

In contrast to the classical case, where implicit and explicit existence proofs of discrete breathers are known [17–20], and where reliable computational tools are available which allows one to obtain numerical solutions on large lattices [11], the situation with the quantum case is different. Except for some integrable one-dimensional models no analytical solutions are known. Numerical evaluations will have to face the tremendous problem of diagonalizing large matrices even for moderate system sizes (like 6-10 sites). In order to gain an insight into the problem it is useful to study

small systems where the discrete breather concept can be partially used. Although there is no localization length anymore, we may still find excitations which are mainly located on one site. The smallest possible system is thus a two site system, i.e. a dimer. For $\delta = 0$ equation (1.1) describes an integrable dimer. The analysis of this model [8] demonstrates that the existence of classical discrete breather solutions corresponds to the appearance of tunneling pairs of eigenstates. These pairs of eigenstates have energy splittings which are orders of magnitude smaller than the averaged level spacing. The relative splittings decrease with the increase of the eigenenergies, in full correspondence with the above described expectations.

One nongeneric feature of the dimer model is its integrability. Although it allowed to obtain analytical results, it could hide some features of the generic nonintegrable case. This conclusion led to the consideration of the trimer model. The third site was deliberately chosen to be different from the first two sites in order to preserve the symmetries of the model. Some classical and quantum properties of (1.1) were described in detail in a previous paper [7]. The discussion of the classical properties was devoted mainly to periodic orbit bifurcations which allow for an appearance of discrete breather solutions transforming into each other under the $1 \leftrightarrow 2$ permutation in the trimer. In the quantum case we again observe pairs of symmetric and antisymmetric states with nearly coinciding energy levels. Note that the energy splitting in such pairs is determined by the phase space tunneling amplitude between the above two classical solutions.

The paper [7] presents data on the behavior of such pairs as well as of individual levels with varying coupling parameter δ . We observe that pairs can be crossed by other pairs and/or by individual levels. The crossing for levels with the same symmetry is certainly avoided whereas levels with differing symmetries really cross each other. In many cases a pair is able to survive many crossings and restore itself up to large values of δ . However, sooner or later a fatal crossing comes which destroys the pair. In the classical system this loss is manifested by a strong overlap of the corresponding quantum wave function with chaotic layers in the phase space of the classical model.

The level splittings were not analyzed in more detail. Instead only their behaviour on scales comparable with the averaged level spacing were of interest. Here we will present a careful analysis of the mighty changes of the tiny splittings as the coupling δ is changed. Denote with x, y, z the eigenvalues of the site number operators n_1, n_2, n_3 . We may consider the quantum states of the trimer at $\delta = 0$ when z is a good quantum number and then follow the evolution of these states with increasing δ . The state for $\delta = 0$ can be traced back to $C = 0$ and be thus characterized in addition by x and y .

II. TUNNELING ORDER, MAGNITUDE AND RESONANCES

In Fig. 2(b) in the previous paper [7] we picked a tunneling pair which has energy ≈ 342 for $\delta = 0$. The fixed model parameters were $B = 40$ and $C = 2$. The pair states are characterized by $x = 26(0)$, $y = 0(26)$ and $z = 14$ for $C = \delta = 0$. Note that this pair survives approximately 30 avoided crossings before it finally is destroyed at coupling strength $\delta \approx 2.67$.

Figure 1 presents the dependence of the tunneling splitting, ΔE , for this pair. One sees that the splitting rapidly

increases gaining about eight orders of magnitude when δ changes from 0 to slightly above 0.5. Then this rapid but nevertheless smooth rise is interrupted by very sharp spikes when the splitting ΔE rises by several orders of magnitude with δ changing by mere percents and then abruptly changes in the opposite direction sometimes even overshooting its prespike value. Such spikes, some larger, some smaller, repeat with increasing δ until the splitting value approaches the mean level spacing (of order one in the figure). Only then one may say that the pair is destroyed since it can be hardly distinguished among the other trimer levels.

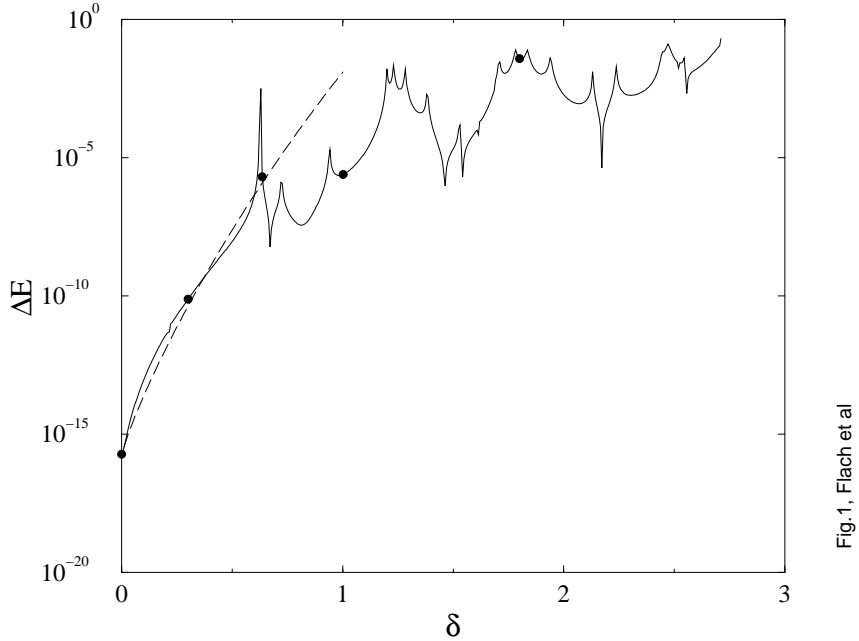


Fig.1, Flach et al

FIG. 1. Level splitting versus δ for level pair as described in the text. Solid line - numerical result. Dashed line - semiclassical approximation as described in text. Filled circles - location of wave function analysis in Fig.2.

Another observation is presented in Figs.2 (a-e). We plot the intensity distribution of the logarithm of the squared symmetric wavefunction of our chosen pair for five different values of $\delta = 0, 0.3, 0.636, 1.0, 1.8$ (their locations are indicated by filled circles in Fig.1). We use the eigenstates of B as basis states. They can be formally represented as $|x, y, z\rangle$ where x, y, z are the particle numbers on sites 1, 2, 3, respectively. Due to the commutation of B with H two site occupation numbers are enough if the total particle number is fixed. Thus the final encoding of states (for a given value of b) can be chosen as $|x, z\rangle$ (see also [7] for details). The abscissa in Figs.2 is x and the ordinate is z . Thus the intensity plots provide us with information about the order of particle flow in the course the tunneling process.

Fig.2a, Flach et al

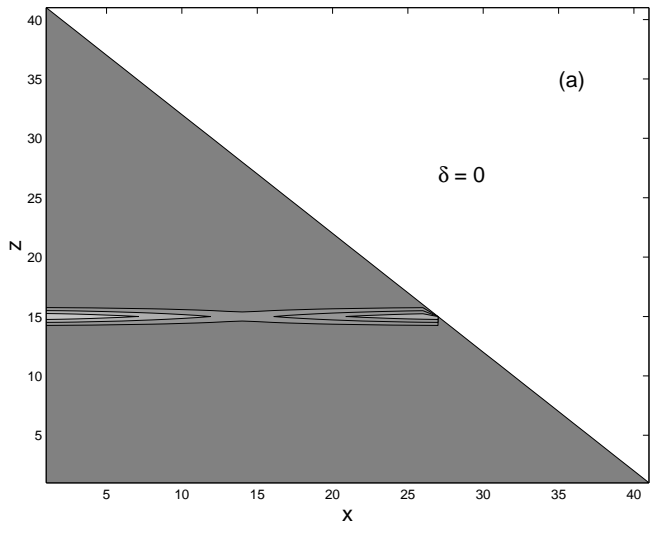


Fig.2b, Flach et al

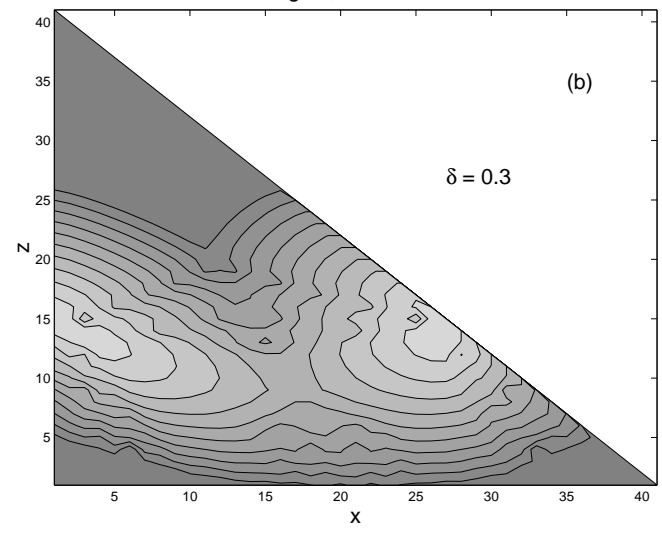


Fig.2c, Flach et al

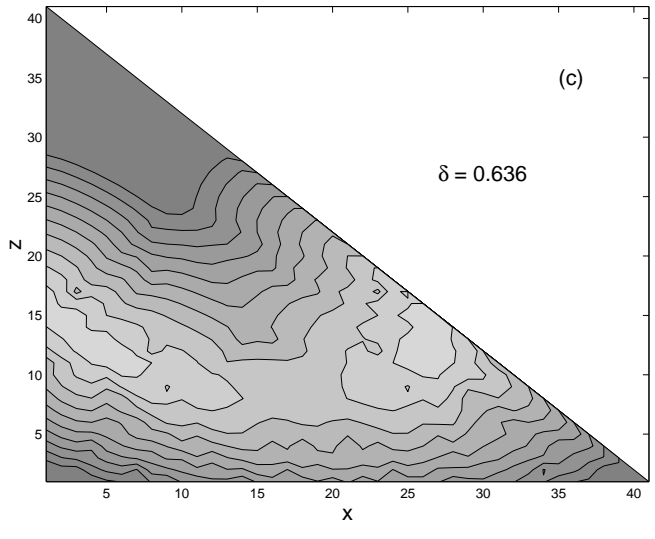
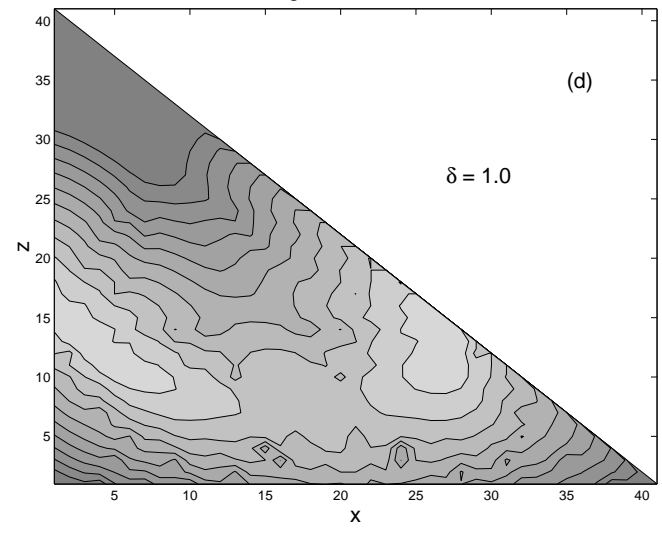


Fig.2d, Flach et al



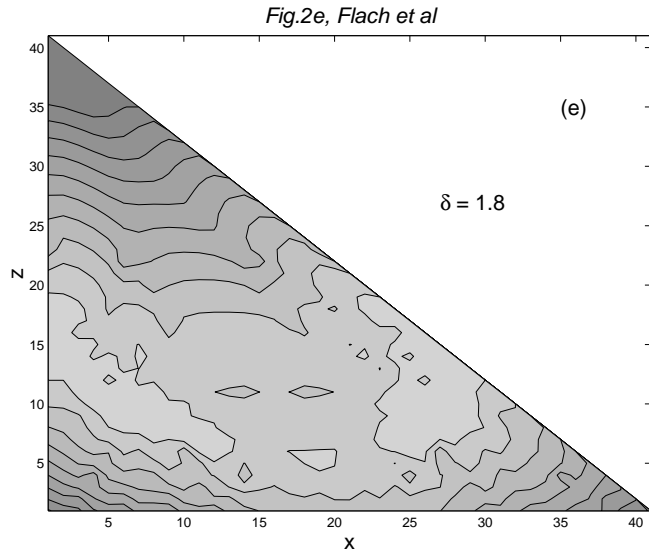


FIG. 2. Contour plot of the logarithm of the symmetric eigenstate of the chosen tunneling pair (cf. Fig.1) for five different values of $\delta = 0, 0.3, 0.636, 1.0, 1.8$ (their location is indicated by filled circles in Fig.1). In Fig.2(a) three equidistant grid lines are used. In Figs.2(b-e) ten grid lines are used. Minimum value of squared wave function is 10^{-30} , maximum value is about 1.

For $\delta = 0$ (Fig.2a) the only possibility for the 26 particles on site 1 is to directly tunnel to site 2. Site 3 is decoupled with its 14 particles not participating in the process. The squared wavefunction takes the form of a compact rim in the (x, z) plane which is parallel to the x axis. Nonzero values of the wavefunction are observed only on the rim. This direct tunneling has been quantitatively described in [8]. When switching on some nonzero coupling to the third site, the particle number on the dimer (sites 1,2) is not conserved anymore. The third site serves as a particle reservoir which is able either to collect particles from or supply particles to the dimer. This coupling will allow for nonzero values of the wavefunction away from the rim. But most importantly, it will change the shape of the rim. We observe that the rim is bended down to smaller z values with increasing δ . That implies that the order of tunneling (when, e.g., going from large to small x values) is as follows: first, some particles tunnel from site 1 to site 2 and simultaneously from site 3 to site 2 (Fig.3(a)). Afterwards particles flow from site 1 to both sites 2 and 3 (Fig.3(b)). With increasing δ the structure of the wavefunction intensity becomes more and more complex, possibly revealing information about the classical phase space flow structure.

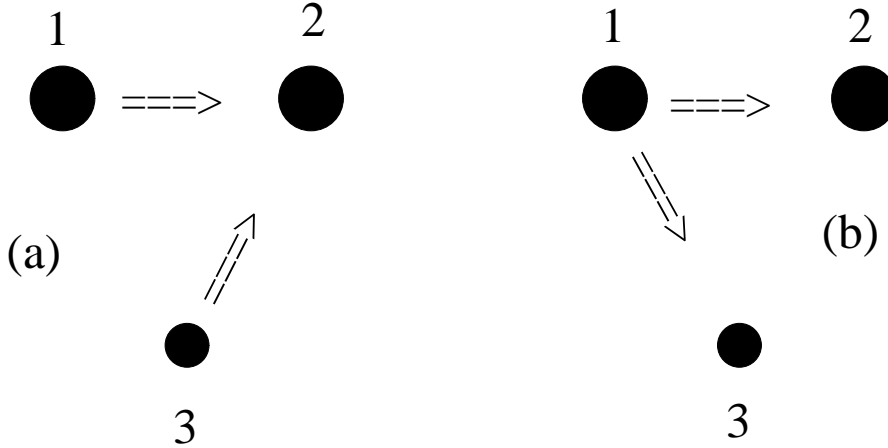


Fig.3 Flach et al

FIG. 3. Order of tunneling in the trimer. Filled large circles - sites 1 and 2, filled small circle - site 3. Arrows indicate direction of transfer of particles.

Thus we observe three intriguing features. First, the tunneling splitting increases by eight orders of magnitude when δ increases from zero to 0.5. This seems to be unexpected, since at those values perturbation theory in δ should be applicable (at least Fig.2b in [7] demonstrates that this should be true for the levels themselves). The second observation is that the tunneling begins with a flow of particles from the bath (site 3) directly to the empty site which is to be filled (with simultaneous flow from the filled dimer site to the empty one). At the end of the tunneling process the initially filled dimer site is giving particles back to the bath site. Again this is an unexpected result, since it implies that the particle number on the dimer is increasing during the tunneling, which seems to decrease the tunneling probability, according to the results for an isolated dimer. These first two results are closely connected, as we will show below. The third result concerns the resonant structure on top of the smooth variation in Fig.1. The resonant enhancements and suppressions of tunneling are related to avoided crossings. Their presence implies that a fine tuning of the system parameters may strongly suppress or enhance tunneling which may be useful for spectroscopic devices. In the following we will explain all three observations.

A. The order of tunneling

To understand the order of tunneling we consider a generalized model Hamiltonian for $C = \delta = 0$

$$H_g = f(n_1) + f(n_2) + g(n_3) . \quad (2.1)$$

It reduces to (1.1) when choosing $f(x) = x^2/2$ and $g(z) = 0$. Switching on some interaction inside the dimer ($C \neq 0$) we will observe some tunneling probability. The smallness of this probability is due to the presence of an energy barrier hindering successive transferring of particles from one site of the dimer to the other. This energy barrier is given by

$$\Delta_b = \max_{0 < x < (b-z_0)} |f(b-z_0) - (f(b-z_0-x) + f(x))| \quad (2.2)$$

where the total number of particles b and the number of particles on the still isolated third site z_0 are fixed. Note that the top of the barrier is reached when the particles are evenly spread inside the dimer (it is straightforward to generalize to other cases).

At nonzero δ the value of z may fluctuate. Now we have to consider the energy in the two-dimensional plane (x, z) . The energy landscape for an arbitrary distribution of particles with respect to the chosen initial distribution $x = 0$, $y = b - z_0$, $z = z_0$ reads

$$\Delta_b(x, z) = |f(x) + f(b - x - z) + g(z) - f(b - z_0) - g(z_0)| \quad . \quad (2.3)$$

For small values of δ the variation of z will be small and we may expand around z_0 : $z = z_0 + \delta z$. As noted above (2.3) has a maximum at $x = (b - z_0)/2$ for fixed z_0 . In general the derivative of this function along z will, however, not vanish in this point. This implies that a variation of z will change the barrier height. We have to determine the sign of the variation δz which lowers the barrier height. This sign will tell us whether the particle number on site 3 will decrease or increase during the tunneling. Thus, we may predict or explain the change of the rim shape of the above described squared wavefunction. This in turn will allow us to conclude about the order of tunneling. Define $e_1 = f(b - z_0) - 2f((b - z_0)/2)$ and $e_2 = f'((b - z_0)/2) - g'(z_0)$. Straightforward arithmetics leads to the result:

$$\delta z > 0 \quad \text{if } [e_1 > 0 \text{ and } e_2 < 0] \text{ or } [e_1 < 0 \text{ and } e_2 > 0] \quad (2.4)$$

$$\delta z < 0 \quad \text{otherwise} \quad (2.5)$$

Our chosen Hamiltonian (1.1) yields $\delta z < 0$ which is in full accord with the observed change of the rim shape in Figs. 2.

The above considerations allow us to conclude that the tunneling enhancement due to the lowering of the barrier is not sensitive to the sign of δz . The only possibility to avoid tunneling enhancement is to choose $e_2 = 0$. Still one will be faced with consideration of higher order contributions of δz to the barrier change.

B. Quantitative account for the tunneling enhancement

Now we present a semiclassical approach which is capable of accounting for the rapid increase of the energy splitting in the tunneling pair shown in Fig.1. For this sake we shall first discuss tunneling in the dimer. Then we will show how the introduction of an interaction with the third site will modify the results.

A semiclassical treatment of tunneling in the dimer was outlined in [16] where canonical coordinates were introduced, using the classical variables $\Psi_l = \sqrt{n_l} e^{i\varphi_l}$,

$$q = \frac{1}{2}[n_2 - n_1], \quad p = \varphi_2 - \varphi_1,$$

$$J = n_1 + n_2, \quad \chi = \frac{1}{2}(\varphi_1 + \varphi_2) \quad . \quad (2.6)$$

These coordinates allow one to represent the dimer Hamiltonian in the form

$$H_d = \left(\frac{J}{2}\right)^2 + q^2 + 2C\sqrt{\left(\frac{J}{2}\right)^2 - q^2} \cos p \quad (2.7)$$

Here the phase p plays the role of a momentum whereas q is the coordinate along which the tunneling in the dimer takes place. The coordinate J is an integral of motion, since the Hamiltonian does not depend on its canonically conjugated momentum χ . In order to calculate the tunneling probability amplitude we first choose two symmetry breaking isolated periodic orbits with a certain energy E and then look for a classical path $q(\tau)$ in the complex time plane which connects these two orbits. On this way we have to cross classically forbidden areas where the momentum p becomes imaginary. What we need to know is the dependence of the momentum p on the coordinate q which, in the classically forbidden area, is determined by the equation

$$E = \left(\frac{J}{2}\right)^2 + q_0^2 + 2C\sqrt{\left(\frac{J}{2}\right)^2 - q_0^2} \cosh p. \quad (2.8)$$

The boundaries $\pm q_0(E)$ of this area or the turning points are obtained from equation (2.8) at $p = 0$ for a given energy E .

The tunneling probability amplitude can be estimated as

$$W \sim \exp\{-S\}$$

where

$$S = \int_{-q_0}^{q_0} p(q) dq. \quad (2.9)$$

This integral can be readily evaluated for the energy $E_3 = J^2/2 + C^2$ (for a given value of J). Then $q_0 = \sqrt{J^2/4 - C^2}$ and

$$S(E = E_3) = -\sqrt{J^2 - 4C^2} + J \ln \left(\frac{2C}{J - \sqrt{J^2 - 4C^2}} \right) \quad (2.10)$$

This expression coincides, to within the preexponential factor, with the results obtained in [16]. However our aim here is to consider the tunneling amplitude of the trimer or, to be more specific, consider how the tunneling splitting for a certain pair of the trimer levels varies with the increase of the coupling parameter δ .

A naive approach is based on equation (2.10). An interaction with the third site of the trimer may lead to a change of the number J of particles in the dimer (first two sites). One can readily see that the action (2.10) becomes larger for larger J values. Since the total number of particles in the trimer is fixed, $b = J + n_3$, an increase of J occurs only at the expense of the third site which may provide the necessary particles. Therefore the tunneling amplitude decreases if n_3 should decrease, and this is completely opposite to what we have observed numerically in the previous section. It means that a more detailed analysis is needed.

First, we introduce canonical coordinates which are explicitly symmetric with respect to permutation of the first two sites of the trimer.

$$Q = \frac{1}{3}(n_1 + n_2) - \frac{2}{3}n_3, \quad \pi = \frac{1}{2}(\varphi_1 + \varphi_2) - \varphi_3,$$

$$b = n_1 + n_2 + n_3, \quad \bar{\chi} = \frac{1}{3}(\varphi_1 + \varphi_2 + \varphi_3). \quad (2.11)$$

The definitions of the two coordinates q and p , related to the dimer, remain as in equation (2.6). Then the trimer Hamiltonian (1.1) takes the form

$$\begin{aligned} H = & \left(\frac{1}{3}b + \frac{1}{2}Q\right)^2 + q^2 + 2C\sqrt{\left(\frac{1}{3}b + \frac{1}{2}Q\right)^2 - q^2} \cos p \\ & + 2\delta\sqrt{\left(\frac{1}{3}b - Q\right)\left(\frac{1}{3}b + \frac{1}{2}Q + q\right)} \cos\left(\pi + \frac{1}{2}p\right) \\ & + 2\delta\sqrt{\left(\frac{1}{3}b - Q\right)\left(\frac{1}{3}b + \frac{1}{2}Q - q\right)} \cos\left(\pi - \frac{1}{2}p\right). \end{aligned} \quad (2.12)$$

It becomes straightforward to obtain equations of motions for the four relevant coordinates, with b being an integral of motion and $\bar{\chi}$ redundant. We need here only two of this equations

$$\begin{aligned} \dot{Q} = & -2\delta\sqrt{\left(\frac{1}{3}b - Q\right)\left(\frac{1}{3}b + \frac{1}{2}Q + q\right)} \sin\left(\pi + \frac{1}{2}p\right) \\ & - 2\delta\sqrt{\left(\frac{1}{3}b - Q\right)\left(\frac{1}{3}b + \frac{1}{2}Q - q\right)} \sin\left(\pi - \frac{1}{2}p\right) \end{aligned} \quad (2.13)$$

$$\begin{aligned} -\dot{\pi} = & \frac{1}{3}b + \frac{1}{2}Q + \frac{C\left(\frac{1}{3}b + \frac{1}{2}Q\right)}{\sqrt{\left(\frac{1}{3}b + \frac{1}{2}Q\right)^2 - q^2}} \cos p + \\ & \delta \cos\left(\pi + \frac{1}{2}p\right) \left[\frac{1}{2}\sqrt{\frac{\left(\frac{1}{3}b - Q\right)}{\left(\frac{1}{3}b + \frac{1}{2}Q + q\right)}} - \sqrt{\frac{\left(\frac{1}{3}b + \frac{1}{2}Q + q\right)}{\left(\frac{1}{3}b - Q\right)}} \right] + \\ & \delta \cos\left(\pi - \frac{1}{2}p\right) \left[\frac{1}{2}\sqrt{\frac{\left(\frac{1}{3}b - Q\right)}{\left(\frac{1}{3}b + \frac{1}{2}Q - q\right)}} - \sqrt{\frac{\left(\frac{1}{3}b + \frac{1}{2}Q - q\right)}{\left(\frac{1}{3}b - Q\right)}} \right]. \end{aligned} \quad (2.14)$$

These equations will allow us to estimate the deviation of the tunneling trajectory in the (q, Q) plane. The latter can be directly mapped onto the (z, x) plane. Again we may consider trajectories connecting isolated periodic orbits with $\dot{p} = \dot{p} = \dot{\pi} = \pi = 0$. A reasonable approximation is to assume that $\dot{\pi} = \pi = 0$ along the path and then use equation (2.13) to estimate the deviation of the Q value from its initial Q_0 values,

$$\Delta Q \sim \dot{Q}_{max} \frac{\Delta\tau}{2} \sim -\frac{\delta\sqrt{Q_0(b/3 - Q_0)}}{\sqrt{2}C} \quad (2.15)$$

Here \dot{Q}_{max} is the largest value of \dot{Q} . It is estimated by substituting $Q = Q_0$, $q = 0$ (the middle point of the tunneling path) and p_{max} into equation (2.13). As for p_{max} it is found for the given dimer energy from equation (2.7) at $q = 0$. $\Delta\tau = 1/\sqrt{J^2/4 - C^2}$ is the time of motion through the forbidden region (traversal time).

First, we again obtain that the tunneling trajectory really deviates towards lower values of Q , i.e. towards a decreasing number z of bosons in the third site. It fits our numerical results. In order to calculate the corresponding action we slightly deform the trajectory. Better to say we straighten the trajectory, which finally simply becomes a straight line with constant z which is shifted towards lower z -values. We believe that this deformation would lead to a negligible change of the result since the deformation is carried out mainly in the borders of the forbidden area. The principal contribution to the integral comes, however, from the central part of this area.

This procedure allows us to return to the calculation of the tunneling amplitude in the dimer by means of the integral (2.9). However, the number of bosons, which has been J in the isolated dimer, becomes now $J' = J + \Delta Q$. As for the energy of the dimer it should remain without change ($E = E_3$), since we neglect small corrections (order of δ^2) due to the interaction with third site. The distance to the upper bound $E'_3 = J'^2/2 + C^4$ can be readily found, $\Delta E \approx J\Delta Q$. There should be also a small shift of the turning points q'_0 which is, however, of a minor importance.

As a result we can represent the action in an integral form

$$S = \int_{-q'_0}^{q'_0} dq \arccos \frac{\frac{J'^2}{4} + \Delta E - q^2}{2C\sqrt{\frac{J'^2}{4} - q^2}} \quad (2.16)$$

This integral can be calculated analytically and in the trivial case of $\Delta Q = 0$ it reduces to equation (2.10). However, the general analytic expression for (ref3-11) is extremely cumbersome. That is why we have preferred to calculate this integral numerically. The thick dashed line in Fig.1 is the graphical form of (2.16). We observe very good agreement with the numerical data for tunneling in the trimer up to δ values where possibly our expansion becomes too crude and where the spiky structure sets in. Yet our consideration is capable of quantitatively describing the raising of the tunneling splitting by eight orders of magnitude!

C. Resonances due to avoided crossings

Let us give a semiquantitative understanding of the spiky behaviour of the energy splitting dependence on δ in Fig.1. Comparing the position of the spikes with the level variation in Fig.2b in [7] we immediately realize that each resonance in Fig.1 is related to an avoided crossing of our level pair with either a single third level or another tunneling pair. A simple analytical description of such crossing can be obtained following the same simple reasoning which has led to the understanding of an avoided crossing of just two levels (see, e.g., [21]).

Let us first assume that we have found all eigenenergies and eigenfunctions of the trimer for given values of the parameters C and δ_0 . We denote the energies and wave function of our tunneling pair as ε_{1s} , ε_{1a} and ψ_{1s} , ψ_{1a} . Here indices s and a relate to the symmetric and antisymmetric states. We also assume that there is a level or another pair of levels which happen to be very close to our tunneling pair. Then we may consider small variations $\tilde{\delta}$ of the coupling parameter δ near its δ_0 value ($\delta = \delta_0 + \tilde{\delta}$) and calculate the variation of the level energies by means of the perturbation theory, neglecting contributions from all other more distant levels. The corresponding perturbation is

explicitly symmetric with respect to the 1 – 2 permutations. Therefore it may mix only the states with the same symmetry, so that those levels will avoid crossings. As for states of different symmetries, their crossing is allowed.

1. Pair — single level crossing

First we consider the case when the tunneling pair is approached by a single level which we choose to be symmetric with respect to the permutation of the dimer sites. The energy and the wave function of this level at $\delta = \delta_0$ are ε_{2s} and ψ_{2s} . Such a crossing can be described by the 3×3 matrix

$$\begin{pmatrix} \varepsilon_{1s} + V_{s11}\tilde{\delta} & V_{s12}\tilde{\delta} & 0 \\ V_{s12}\tilde{\delta} & \varepsilon_{2s} + V_{s22} & 0 \\ 0 & 0 & \varepsilon_{1a} + V_{a11} \end{pmatrix}. \quad (2.17)$$

where all terms proportional to $\tilde{\delta}$ are the corresponding matrix elements of the perturbation. They vanish at δ_0 which is close enough to the avoided crossing.

Diagonalizing the matrix (2.17) we obtain three levels

$$E_{s\{1,2\}} = \frac{\varepsilon_{s1} + \varepsilon_{s2} + (V_{s11} + V_{s22})\tilde{\delta}}{2} \pm \sqrt{\frac{[\varepsilon_{s1} - \varepsilon_{s2} + (V_{s11} - V_{s22})\tilde{\delta}]^2}{4} + V_{s12}^2\tilde{\delta}^2}$$

$$E_a = \varepsilon_{a1} + V_{a11}\tilde{\delta} \quad (2.18)$$

There are two different scenaria which depend on the parameters of the matrix. In the first case at $\delta = \delta_0$ the order of the levels in either increasing or decreasing order is $\varepsilon_{1a}, \varepsilon_{1s}, \varepsilon_{2s}$. In this case we will first see a decrease of the splitting down to zero (!) and a subsequent increase of the splitting up to some maximum with subsequent decrease down to its original value. In the second case $\varepsilon_{2s}, \varepsilon_{1a}, \varepsilon_{1s}$ the above sequence is reversed - we first observe an increase up to a maximum, then a decrease down to zero and a final increase to the original splitting value. All the parameters may be chosen to be positive. The difference between the coefficients V_{s11} and V_{a11} is neglected since this difference reflects the slow change of the level splitting with varying δ (cf. Fig.1). The perturbation theory allows us to deal only with small values of $\tilde{\delta}$, hence parameters should satisfy the conditions that $|\varepsilon_{s1} - \varepsilon_{s2}| \ll |V_{s11} - V_{s22}|$ and $|V_{s12}| \ll 1$.

Then the tunneling splitting Δ can be found as a function of $\tilde{\delta}$. It can be defined as the smallest distance between the antisymmetric level and the two symmetric levels,

$$\Delta = \min\{|E_{s1} - E_a|, |E_{s2} - E_a|\} \quad (2.19)$$

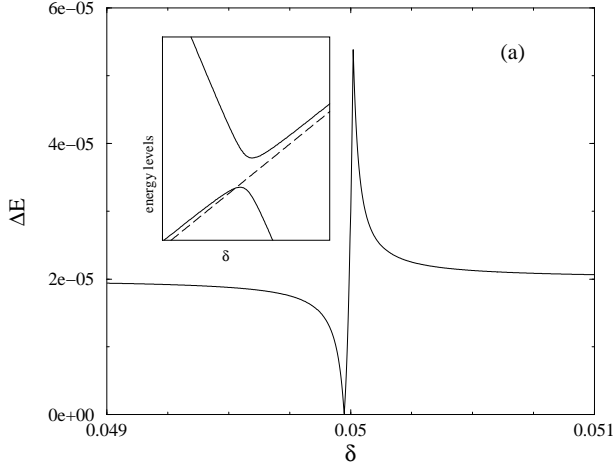


Fig.4a, Flach et al

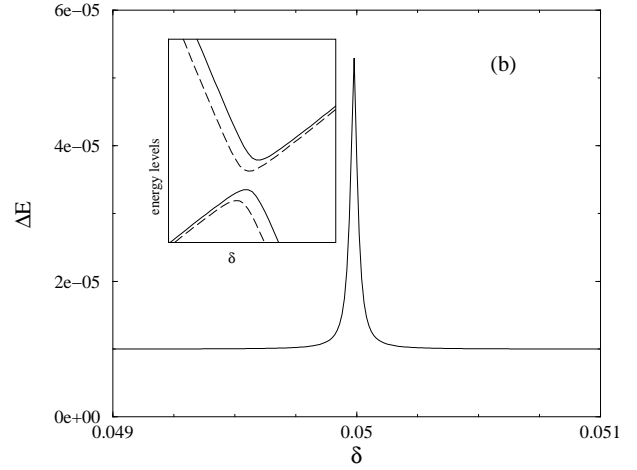


Fig.4b, Flach et al

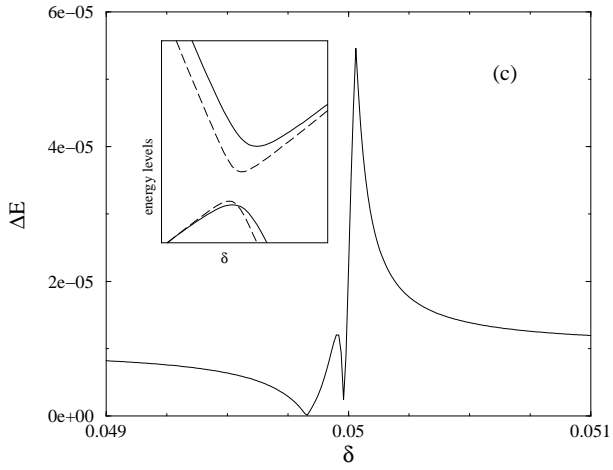


Fig.4c, Flach et al

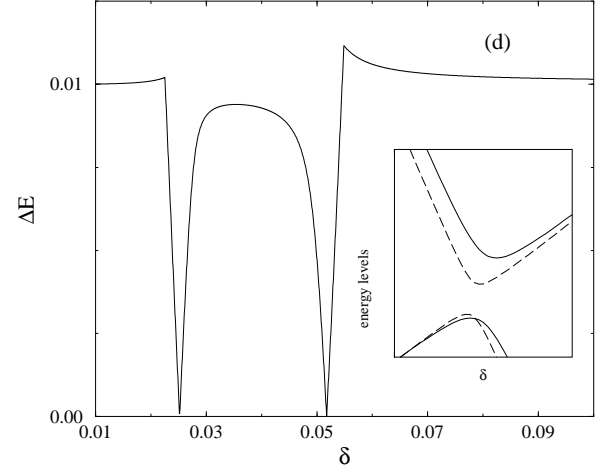


Fig.4d, Flach et al

FIG. 4. Level splitting variation at avoided crossings.

Inset: Variation of individual eigenvalues participating in the avoided crossing. Solid lines - symmetric eigenstates, dashed lines - antisymmetric eigenstates.

An example is shown in Fig.4(a) ($V_{s11} = V_{a11} = 1, V_{s22} = -3, V_{s12} = 0.001, \varepsilon_{s1} = 0.1, \varepsilon_{s2} = 0.3, \varepsilon_{a1} - \varepsilon_{s1} = 0.00002$, the asymmetric level lies below its symmetric counterpart in the tunneling pair.) where Δ is plotted as a function of $\tilde{\delta}$.

Crossing of a tunneling pair with an antisymmetric level is described in a similar manner by the same matrix with interchange of indices s and a .

2. Pair — pair crossing

In order to analyze a pair — pair crossing we should consider two tunneling pairs with the energies $\varepsilon_{s1}, \varepsilon_{a1}$, and $\varepsilon_{s2}, \varepsilon_{a2}$ together with the corresponding wave functions, ψ_{s1}, ψ_{a1} , and ψ_{s2}, ψ_{a2} . Again we assume that these two pairs lie close to each other at $\delta = \delta_0$, so that the perturbation theory can be applied, disregarding all the other states

of the trimer. Then we should consider the matrix

$$\begin{pmatrix} \varepsilon_{1s} + V_{s11}\tilde{\delta} & V_{s12}\tilde{\delta} & 0 & 0 \\ V_{s12}\tilde{\delta} & \varepsilon_{2s} + V_{s22} & 0 & 0 \\ 0 & 0 & \varepsilon_{a1} + V_{a11}\tilde{\delta} & V_{a12}\tilde{\delta} \\ 0 & 0 & V_{a12}\tilde{\delta} & \varepsilon_{a2} + V_{a22}\tilde{\delta} \end{pmatrix}. \quad (2.20)$$

whose diagonalization results in four energies

$$E_{s\{1,2\}} = \frac{\varepsilon_{s1} + \varepsilon_{s2} + (V_{s11} + V_{s22})\tilde{\delta}}{2} \pm \sqrt{\frac{[\varepsilon_{s1} - \varepsilon_{s2} + (V_{s11} - V_{s22})\tilde{\delta}]^2}{4} + V_{s12}^2\tilde{\delta}^2} \quad (2.21)$$

$$E_{a\{1,2\}} = \frac{\varepsilon_{a1} + \varepsilon_{a2} + (V_{a11} + V_{a22})\tilde{\delta}}{2} \pm \sqrt{\frac{[\varepsilon_{a1} - \varepsilon_{a2} + (V_{a11} - V_{a22})\tilde{\delta}]^2}{4} + V_{a12}^2\tilde{\delta}^2}$$

We may now construct four possible differences between the energies of two symmetric and two antisymmetric states which give us possible splittings. Then choosing the difference with the lowest absolute value we define the tunneling splitting Δ at a given value of the parameter δ . The choice of other parameters in equations (2.21) is governed by the similar principles as in the pair — single level crossing.

There are at least three different scenaria which may appear. The first two are realized when the interaction between the two symmetric and the two antisymmetric states is much stronger than the interaction inside each pair which yields the individual pair splittings. If $V_{s12} \approx V_{a12}$ the avoided crossing results in a simple resonance of the splitting (Fig. 4(b) , parameters $\varepsilon_{s1} = 0.1$, $\varepsilon_{s2} = 0.3$, $\varepsilon_{a1} = 0.09999$, $\varepsilon_{a2} = 0.2999$, $V_{s11} = V_{a11} = 1$, $V_{s22} = V_{a22} = -3$, $V_{s12} = V_{a12} = 0.001$).

If the symmetric states are interacting stronger (or weaker) than their antisymmetric counterparts $V_{s12} \neq V_{a12}$, two intersections inside one of the two pairs are possible (Fig. 4(c), parameters $\varepsilon_{s1} = 0.1$, $\varepsilon_{s2} = 0.3$, $\varepsilon_{a1} = 0.09999$, $\varepsilon_{a2} = 0.2999$, $V_{s11} = V_{a11} = 1$, $V_{s22} = V_{a22} = -3$, $V_{s12} = 0.002$, $V_{a12} = 0.001$).

Finally, if the interaction between the two symmetric and the two antisymmetric states is much weaker than the interaction inside each pair, the pairs will intersect each other and the avoided crossing structure will appear on a finer scale than the pair splittings. An example is shown in Fig. 4(d) (parameters $\varepsilon_{s1} = 0.1$, $\varepsilon_{s2} = 0.3$, $\varepsilon_{a1} = 0.09$, $\varepsilon_{a2} = 0.2$, $V_{s11} = V_{a11} = 1$, $V_{s22} = V_{a22} = -3$, $V_{s12} = V_{a12} = 0.1$).

III. CONCLUSION

We have described and explained peculiar features of dynamical tunneling of a strong excitation in a trimer. The tunneling amplitude may be enhanced due to the presence of the third site with fluctuating particle number. Numerical calculations show that this amplitude grows about eight orders of magnitude when the coupling parameter δ still remains much smaller than all other parameters in the system. An interesting feature of this process is that the third site serves as a donor which injects bosons into the dimer and thus speeds up tunneling. The injected bosons are

of course returned to the third site at the end of the tunneling process. Such a process thus needs a nonzero amount of bosons to be deposited on the third site at the beginning of tunneling.

It is worthwhile to compare the observed enhancement of tunneling with our consideration of a tunneling of a breather in a one-dimensional chain [16]. The result of that paper was that the interaction of the dimer with other degrees of freedom in the chain may result only in a reduction of the tunneling amplitude. This finding was in agreement with studies of dissipative tunneling [2,3]. The reason for the opposite result in the present work is that we consider a situation in which the third harmonic site is excited to a rather high level and is able to provide bosons necessary to enhance the tunneling. This is in contrast to the above references where the temperature was assumed to be zero or low, meaning that the bath degrees of freedom were not excited.

Note that the discussion in Subsection II.A prompts a possibility of a tunneling enhancement even at zero occupation of the third site. This can be achieved in our model by choosing $g(n_3) = \omega_3 n_3$ with $\omega_3 > B/2$. Again the expected enhancement of tunneling is opposite to the above statement and is due to the choice of such a large value of the frequency ω_3 of the third site which makes the adiabatic approximation [16] invalid. It means that the shape of the instanton calculated in [16] may be significantly altered by the interaction with this high frequency mode.

The spikes observed in the δ dependence of the tunneling amplitude are well explained by the relevant crossings with either single levels or with other tunneling pairs of levels. At higher values of δ when the tunneling splitting comes close to average level spacing (1 in our model) the whole picture becomes more complicated and one may think about an increasing role of chaos assisted tunneling [1]. However, discussion of this process goes beyond the framework of this paper.

Acknowledgements.

We thank D. Delande, E. Jeckelmann and Y. Zolotaryuk for helpful discussions.

-
- [1] O. Bohigas, S. Tomsovic, and D. Ullmo. Manifestations of classical phase space structures in quantum mechanics. *Phys. Rep.*, 223:43, 1993.
- [2] A. J. Leggett, S. Chakravarty, A. T. Dorsey, M. P. A. Fisher, A. Garg, W. Zwerger. Dynamics of the dissipative 2-state system. *Rev. Mod. Phys.* 59:1, 1987
- [3] U. Weiss. *Quantum dissipative systems* World Scientific, Singapore, 1999
- [4] M. Wilkinson. Tunneling between tori in phase space. *Physica D*, 21:341, 1986.
- [5] M. Wilkinson and J. H. Hannay. Multidimensional tunneling between excited states. *Physica D*, 27:201, 1987.
- [6] A. A. Ovchinnikov, N. S. Erikhman About localization of vibrational energy for highly excited states. *Vibrational excitons. Sov.Phys.Uspekhi*, 25:737, 1982
- [7] S. Flach and V. Fleurov. Tunneling in the nonintegrable trimer - a step towards quantum breathers. *J. Phys.: Cond. Mat.*, 9:7039, 1997.
- [8] S. Aubry, S. Flach, K. Kladko, and E. Olbrich. Manifestation of classical bifurcation in the spectrum of the integrable quantum dimer. *Phys. Rev. Lett.*, 76:1607, 1996.
- [9] D. A. Garanin. Spin tunneling - a perturbative approach. *J. Phys. A*, 24:L61, 1991.
- [10] D. A. Garanin, E. M. Chudnovsky, and R. Schilling. Tunneling of a large spin via hyperfine interactions. *Phys. Rev. B*, 61:12204, 2000.
- [11] S. Flach and C. R. Willis. Discrete breathers. *Phys. Rep.*, 295:181, 1998.
- [12] J. A. Sepulchre and R. S. MacKay. Localized oscillations in conservative or dissipative networks of weakly coupled autonomous oscillators. *Nonlinearity*, 10:679, 1997.
- [13] R. S. MacKay. Discrete breathers: classical and quantum. *Physica A*, in press, 2000.
- [14] W. Z. Wang, J. Tinka Gammel, A. R. Bishop, and M. I. Salkola. Quantum breathers in a nonlinear lattice. *Phys. Rev. Lett.*, 76:3598, 1996.
- [15] W. Z. Wang, A. R. Bishop, J. T. Gammel, and R. N. Silver. Quantum breathers in electron-phonon systems. *Phys. Rev. Lett.*, 80:3284, 1998.
- [16] V. Fleurov, R. Schilling, and S. Flach. Tunneling of a quantum breather in a one-dimensional chain. *Phys. Rev. E*, 58:339, 1998.
- [17] R. S. MacKay and S. Aubry. Proof of existence of breathers for time-reversible or hamiltonian networks of weakly coupled oscillators. *Nonlinearity*, 7:1623, 1994.
- [18] S. Flach. Existence of localized excitations in nonlinear hamiltonian lattices. *Phys. Rev. E*, 51:1503, 1995.
- [19] R. Livi, M. Spicci, and R. S. MacKay. Breathers on a diatomic fpu chain. *Nonlinearity*, 10:1421, 1997.
- [20] C. Baesens and R. S. MacKay. Exponential localization of linear response in networks with exponentially decaying coupling. *Nonlinearity*, 10:931, 1997.
- [21] L. D. Landau and E. M. Lifshitz. *Quantenmechanik, Lehrbuch der Theoretischen Physik III*. Akademie-Verlag Berlin, 1991.